MULTIBODY DYNAMICS 2005, ECCOMAS Thematic Conference
J.M. Goicolea, J.Cuadrado, J.C.García Orden (eds.)
Madrid, Spain, 21–24 June 2005

# A MULTIBODY DYNAMIC MODEL OF A CARDAN JOINT WITH EXPERIMENTAL VALIDATION

**M. Cavacece[†], R. Stefanelli[*], P.P. Valentini [*], L. Vita[*]**

[*] Department of Mechanical Engineering
University of Rome Tor Vergata
Via del Politecnico, 1 – 00133 Rome, Italy
e-mail: `vita@ing.uniroma2.it`

[†] Department of Structural Engineering
University of Cassino
Via Di Biasio, 43 - 03043 Cassino, Italy

**Keywords:** multibody system dynamics, mechanical efficiency, dual algebra, clearance and dimensional tolerances.

**Abstract.** *This investigation deals with the mechanical efficiency of Cardan joints. The model includes also the effects due to manufacturing and mounting errors and the influence of rotation speed and angular configuration of the Cardan joint on the efficiency. The joint has been modeled as an RCCC spatial linkage and the full dynamic analysis has been performed. The equations of motion have been deduced by means both of dual vectors algebra and of classic multibody approach. The results have been compared with experimental ones.*

## 1 INTRODUCTION

Cardan joints are common devices for transmitting the motion between misaligned intersecting axes. A complete dynamic analysis has been presented in a series of papers authored by F. Freudenstein and his coworkers [1,2,3]. However in the mentioned references, friction is not included. For what concerns the mechanical efficiency analysis of Cardan joints the first contribution is due to Morecki [4]. That model included only the losses in the yoke bearings. Considering the widespread industrial applications of Cardan joints, the design of these mechanical devices has to be conducted very carefully. For this reason it is important to investigate the effects of manufacturing errors, misalignments and clearances on the performances of the joints. In this investigation the authors present a complete model of a Cardan joint taking into account both the effects of friction and the effects of mounting errors in all the kinematic pairs. In order to take into account also the effects of misalignment between the axes of two consecutive kinematic pairs, the Cardan joint has been modeled as an RCCC mechanism. A mechanical efficiency analysis based on this model has been developed. The obtained results have been compared to those coming from the experimental test rig equipped at the laboratory of the Department of Mechanical Engineering of University of Rome Tor Vergata. The proposed methodology reveals as an useful tool for the designer to predict the mechanical performances of Cardan joints in real working condition. The influence of angular velocity and output shaft configuration on mechanical efficiency has been also investigated.

## 2 FRICTION MODELLING

In ideal working condition the resultant of the reaction forces at the kinematic pairs is null. This is not necessarily true in presence of radial clearance or manufacturing tolerances. If the presence of friction is considered, frictional forces (moments) arise along (about) the axis of the kinematic pair [5,6]. In order to completely model the effects of friction it is necessary to define the geometric features of the journal bearing.

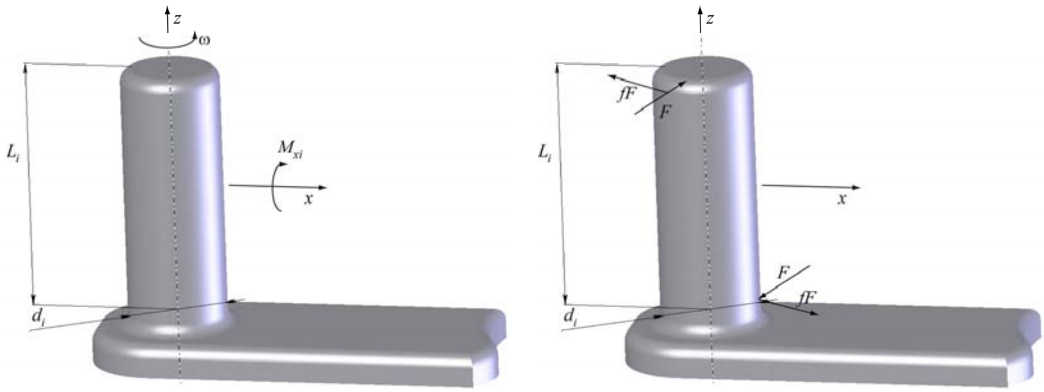


Figure 1: Modelling of friction in revolute joint.

### 2.1 Revolute joint

The frictional forces are mainly caused by the reaction forces ($F_{xi}, F_{yi}, F_{zi}$) and the reaction moments ($M_{xi}, M_{yi}$) at the kinematic pair. The effect of $F_{zi}$ could be neglected considering that there is no sliding velocity along the axis of the revolute joint. In particular the effect of reaction moments could be taken into account considering the equivalent couple of forces (Figure 1):

$$F = \frac{M_{xi}}{L_i}, \tag{1}$$

where $F$ are orthogonal to the direction of $z$ axis.

Thus the frictional torque due to the reaction moment $M_{xi}$ could be evaluated as follow

$$\tau_f^{xi} = f\,\frac{M_{xi}}{L_i} d_i, \tag{2}$$

where $f$ is the friction coefficient, $d_i$ is the diameter of the journal bearing and $L_i$ is the length of the bearing. In the same way the frictional torque due to $M_{yi}$ can be evaluated. Therefore the whole frictional torque about the axis of the journal bearing is

$$M_{zi} = -\text{sign}(\dot{\theta}_i)\left(\tau_f^{(i)} + \frac{fd_i}{2}\sqrt{F_{xi}^2 + F_{yi}^2}\right), \tag{3}$$

where $\dot{\theta}_i$ is the relative angular speed of the journal w.r.t. the bearing and

$$\tau_f^{(i)} = \sqrt{\left(\tau_f^{xi}\right)^2 + \left(\tau_f^{yi}\right)^2}\,. \tag{4}$$

### 2.2 Cylindrical joint

Following the same methodology illustrated for the revolute joint, the frictional moment can be evaluated. In this case a frictional force along the axis of the kinematic pair is also present. Its value is defined by the following equation

$$F_{zi} = -\mathrm{sign}(\dot{s}_i)\, f \left( \sqrt{F_{xi}^2 + F_{yi}^2} + 2\frac{\sqrt{M_{xi}^2 + M_{yi}^2}}{L_i} \right), \tag{5}$$

where $\dot{s}_i$ is the sliding velocity along the $z$ axis.

## 3 DYNAMIC ANALYSIS

The Cardan joint has been modeled as an RCCC mechanism for two main reasons [1,2]. The first one is to simplify the equations of motion avoiding redundant constraints, the second reason is to model clearances and axes misalignments in the kinematic pairs preserving the mobility of the whole mechanism. The dynamic analysis has been performed by means of two different approaches. The first is the classical multibody approach, based on the systematic formulation of the constraint equations as proposed by E. J. Haug in his textbook [7], in order to investigate the influence of angular velocity and output configuration of the Cardan joint on its mechanical efficiency.

The second is the dual algebra approach with the Denavit – Hartenberg method [8,9,10,11], in order to investigate the effects of dimensional tolerances on the mechanical efficiency. This last model was also validated by means of experimental tests. For both of the simulations the inertial and geometric features of the Cardan joint are the same of the one used in the laboratory of the Department of Mechanical Engineering of University of Rome Tor Vergata. In particular in Table 1 the tensor of inertia and static moments, expressed in the local reference frame coordinates, of each element are summarized.

| | Tensor of Inertia [kg m$^2$] | Static Moments [kg m] | Mass [kg] |
|---|---|---|---|
| **Input Shaft** | $\begin{bmatrix} 0.019254 & 0 & 0 \\ 0 & 0.000252 & -0.001026 \\ 0 & -0.001026 & 0.019182 \end{bmatrix}$ | $S_x = 0.11981274$<br>$S_y = 0.008019648$<br>$S_z = 0.119544048$ | 0.936 |
| **Spider** | $\begin{bmatrix} 0.000006 & 0 & 0 \\ 0 & 0.000006 & 0 \\ 0 & 0 & 0.000002 \end{bmatrix}$ | $S_x = 0.000387$<br>$S_y = 0.000387$<br>$S_z = 0$ | 0.0456 |
| **Output Shaft** | $\begin{bmatrix} 0.012147 & 0 & 0 \\ 0 & 0.012148 & 0 \\ 0 & 0 & 0.000184 \end{bmatrix}$ | $S_x = 0.087779952$<br>$S_y = 0.087779952$<br>$S_z = 0$ | 0.936 |

Table 1: Inertial features of the Cardan joint

For the location of the local reference frame of each body see Figure 2.

Figure 2: Location of the local reference frames

The journal bearings between the input (output) shaft and the frame have length *L=0.01* m and diameter *d=0.02* m; the journal bearings between the input (output) shaft and the spider have length *L=0.006* m and diameter *d=0.005* m.

### 3.1 Multibody model

According to the systematic deduction of constraint equations proposed by E. J. Haug [7], the following differential algebraic equations system describes the dynamics of the Cardan joint

$$\begin{cases} [M]\{\ddot{q}\}+\left[\Psi_q\right]^T\{\lambda\}=\{F_e\} \\ \{\Psi(q,t)\}=0 \end{cases}, \tag{6}$$

where $[M]$ represents the global mass matrix, $\{q\}$ the generalized coordinates (seven for each body: three for the location of the centre of mass of the body and four Euler parameters for the attitude), $\left[\Psi_q\right]$ the Jacobian matrix of the constraint equations $\{\Psi(q,t)\}$, $\{\lambda\}$ the Lagrange multipliers and $\{F_e\}$ the generalized external forces. The system (6) is solved by means of the *Radau5* code implemented by E. Hairer, G. Wanner [12]. For this reason it is rearranged into

$$[K]\{\dot{y}\}=\{\phi(y)\}, \tag{7}$$

where

$$[K]=\begin{bmatrix} I & 0 & 0 & 0 \\ 0 & I & 0 & 0 \\ 0 & 0 & 0 & 0 \\ 0 & 0 & 0 & 0 \end{bmatrix} \qquad \{y\}=\begin{Bmatrix} q \\ \dot{q} \\ \ddot{q} \\ \lambda \end{Bmatrix} \qquad \{\phi(y)\}=\begin{Bmatrix} \{\dot{q}\} \\ \{\ddot{q}\} \\ \left\{[M]\{\ddot{q}\}+\left[\Psi_q\right]^T\{\lambda\}-\{F_e\}\right\} \\ \{\Psi\} \end{Bmatrix}$$

In order to take into account the effects of friction it is necessary to evaluate the reaction forces and moments at the kinematic pairs. Thus, solving the equations of motion for $\{\lambda\}$, it is possible to express the reaction forces and moments in the joint reference frame components as

$$\left\{F_i^k\right\}^{(ik)}=-\left[C^T\right]_{ik}^{i}\left[A^T\right]_i^0\left[\Psi_{r_i}\right]^T\{\lambda\} \tag{8}$$

for the reaction forces and

$$\left\{T_i^{ik}\right\}^{(ik)} = \left[C^T\right]_{ik}^{i} \left[\tilde{s}_{p_k}^{(i)}\right]^T \left[A^T\right]_i^0 \left[\Psi_{r_i}\right]^T \{\lambda\} - \frac{1}{2}\left[C^T\right]_{ik}^{i} \left[G\right]_i^0 \left[\Psi_{p_i}\right]^T \{\lambda\} \tag{9}$$

for the reaction moments.

In the expressions (8) and (9) $\left[C^T\right]_{ik}^{i}$ represents the transform matrix from the local frame to the joint frame; $\left[A^T\right]_i^0$ is the transform matrix from the inertial frame to the local one; $\left[\Psi_{r_i}\right]$ and $\left[\Psi_{p_i}\right]$ are the Jacobian matrix of the constraint equations w.r.t. the Cartesian coordinates and Euler parameters respectively; $\left[\tilde{s}_{p_k}^{(i)}\right]$ is the skew matrix of the location vector of the reaction force in local coordinates. Once known the reaction forces and moments, it is possible to evaluate the frictional torque and force at each kinematic pair by means of equations (3) and (5). The effects of friction on the dynamics of the system are evaluated by introducing the frictional forces and torques as external forces into (6). For a correct analysis at each time step one has to evaluate the Lagrange multipliers, then the reactions and the frictional actions and introduce them into the equations of motion for evaluating again the Lagrange multipliers and restart the procedure till convergence. In order to simplify the process, considering that the solution of system (6) is not an easy task, choosing a little time step $\Delta t = 0.0001$ s, the reactions evaluated at time $t$ have been used to compute the frictional torques and forces at time $t + \Delta t$. This approximation does not affect the correctness of the results in a sensitive way but simplify the evaluation process avoiding convergence problems.

### 3.2 Dual algebra approach

This second model of the Cardan joint has been implemented by means of dual algebra. This approach reveals suitable for the description and the analysis of dimensional tolerances and clearances using a small set of equations. Thus the effects of mounting errors on the mechanical efficiency of the Cardan joint has been investigated. Before deducing the equations of motion in terms of dual algebra, some theoretical recalls are herein presented.

By introducing the dual vector as

$$\hat{V} = \vec{v} + \varepsilon \vec{w} \tag{10}$$

where $\vec{v}$ is the geometrical vector, $\varepsilon$ is the dual operator $\left(\varepsilon^2 = 0\right)$ and $\vec{w}$ is the moment of vector $\vec{v}$ w.r.t a chosen point, it is possible to define the *velocity screw* and the *wrench on a screw*. The analytical expression of the velocity screw is

$$\hat{V} = \left(\omega + \varepsilon v\right)\vec{u} \tag{11}$$

where $\omega\vec{u}$ is the angular velocity and $v\vec{u}$ represents the sliding velocity along the rotation axis. Thus the velocity screw describes the kinematic features of a screw motion.

The analytical expression of the wrench on a screw is

$$\hat{F}_A = \vec{F}_A + \varepsilon \vec{C}_A \tag{12}$$

where $\vec{F}_A$ is the resultant of external forces and $\vec{C}_A$ is the resultant moment of the external forces w.r.t. a point $A$ belonging to the central axis[1]. Thus the wrench on a screw represents the resultant of the dynamic action on a body.
Another dual entity useful for this investigation is the dual angle between two axes in space

$$\hat{\theta} = \theta + \varepsilon s \tag{13}$$

where $\theta$ is the geometrical angle, $\varepsilon$ is the dual operator and $s$ is the minimum distance between the axes. The application of trigonometric functions to the dual angle in (13) leads to

$$\begin{aligned} \sin\hat{\theta} &= \sin\theta + \varepsilon s\cos\theta \\ \cos\hat{\theta} &= \cos\theta - \varepsilon s\sin\theta \\ \tan\hat{\theta} &= \tan\theta + \varepsilon s\left(1+\tan^2\theta\right) \end{aligned} \tag{14}$$

and all the properties of the classical algebra are still valid.

The dynamic equations of the Cardan joint, modelled as an RCCC mechanism (see Figure 3), are deduced by means of the dual momentum and the Denavit – Hartenberg formulation. The expression of the dual momentum is

$$\left\{\hat{H}_{C(i)}\right\}^{(i_k)} = m_i\left\{v_{C(i)}\right\}^{(i_k)} - m_i\left[\tilde{R}^{(i_k)}\right]\left\{\omega_i\right\}^{(i_k)} + \varepsilon\left(m_i\left[\tilde{R}^{(i_k)}\right]\left\{v_{C(i)}\right\}^{(i_k)} + \left[J_{C(i)}^{(i_k)}\right]\left\{\omega_i\right\}^{(i_k)}\right) \tag{15}$$

where the real part represents the momentum and the dual one the angular momentum w.r.t. a point *C(i)*. By differentiating (15) w.r.t. time one obtains the dual expression of the equations of motion

$$\frac{d}{dt}\left\{\hat{H}_{C(i)}\right\}^{(i_k)} = \left\{\hat{F}_{C(i)}\right\}^{(i_k)} \tag{16}$$

where $\left\{\hat{F}_{C(i)}\right\}^{(i_k)}$ is the wrench on a screw at each kinematic pair of each moving link.
Considering the equilibrium condition at the kinematic pairs, one obtains

$$\begin{aligned} \left[\hat{A}\right]_1^2\left\{\hat{R}_{C_1}\right\}^{(1)} - \left\{\hat{R}_{C_2}\right\}^{(2)} &= \left\{\hat{F}_{C_2}\right\}^{(2)} \\ \left[\hat{A}\right]_2^3\left\{\hat{R}_{C_2}\right\}^{(2)} - \left\{\hat{R}_{C_3}\right\}^{(3)} &= \left\{\hat{F}_{C_3}\right\}^{(3)} \quad , \\ \left[\hat{A}\right]_3^4\left\{\hat{R}_{C_3}\right\}^{(3)} - \left\{\hat{R}_{C_4}\right\}^{(4)} &= \left\{\hat{F}_{C_4}\right\}^{(4)} \end{aligned} \tag{17}$$

where $\left[\hat{A}\right]_i^{i+1}$ is the dual transform matrix from the local reference system on link $i$ to the local one on link $i+1$ and $\left\{\hat{R}_{C_i}\right\}^{(i)}$ are the dual reactions expressed in the reference frame of link $i$ ($^{(i)}$) w.r.t. a point $C_i$ of the central axis of link $i$. Substituting (17) into (16) one obtains the equations of motion in terms of dual reaction forces. For more details on how to evaluate the expression illustrated see [10,11].

[1] The axis of the resultant of the external forces.

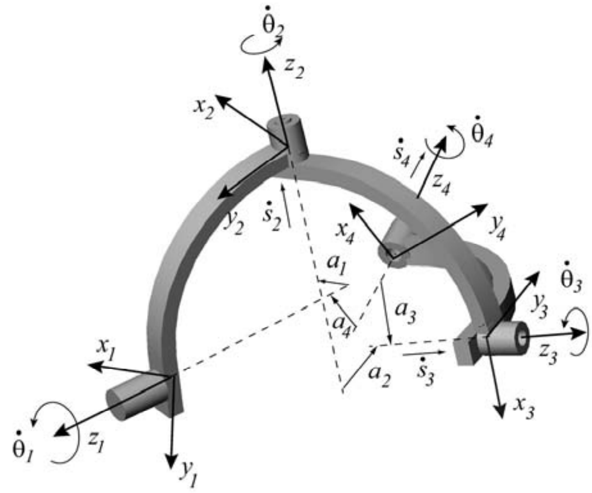

Figure 3: Geometric and kinematic parameters of the RCCC model

Thus the dual reaction forces evaluated by means of (16) are used to compute the dual frictional forces at the kinematic pairs using (3) and (5).

## 4 MECHANICAL EFFICIENCY ANALYSIS

The instantaneous mechanical efficiency of the RCCC mechanism for both of the approaches illustrated is deduced by the following expression

$$\eta_i = \frac{P_{out}}{P_{in}} = \frac{P_{in} - P_{loss}}{P_{in}} = 1 - \frac{P_{loss}}{P_{in}} \tag{18}$$

where $P_{loss}$ is the power loss at the kinematic pairs and $P_{in} = T_{in}\omega_{in}$ is the input power. The power loss could be easily evaluated multiplying the frictional force by the sliding velocity along the axis of the cylindrical joint and the frictional moment by the angular velocity about the axis of the cylindrical / revolute joint.

### 4.1 Multibody approach results

The first kind of analysis conducted refers to the influence of the input / output angular configuration on the mechanical efficiency.

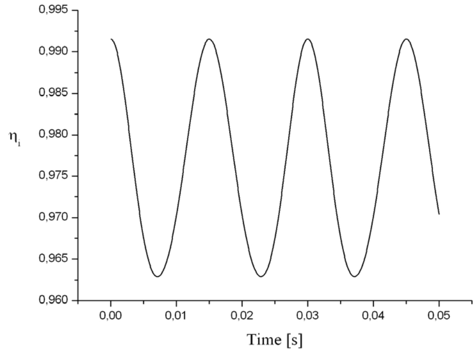


Figure 4: Mechanical efficiency at 10 deg

The parameter chosen for this investigation are:

- Angular configuration of the Cardan joint (which is the angle between input and output shaft): 10 deg.
- Input angular velocity (kept constant) 2000 r.p.m.
- Input torque 2 Nm.
- Coefficient of friction at the kinematic pairs of the spider $f_1=0.42$; coefficient of friction at the kinematic pairs of the shafts $f_2=0.20$.

In Figure 4 the plot of the instantaneous mechanical efficiency versus time is reported. The average value is $\eta_i^{mean} = 0.977$.

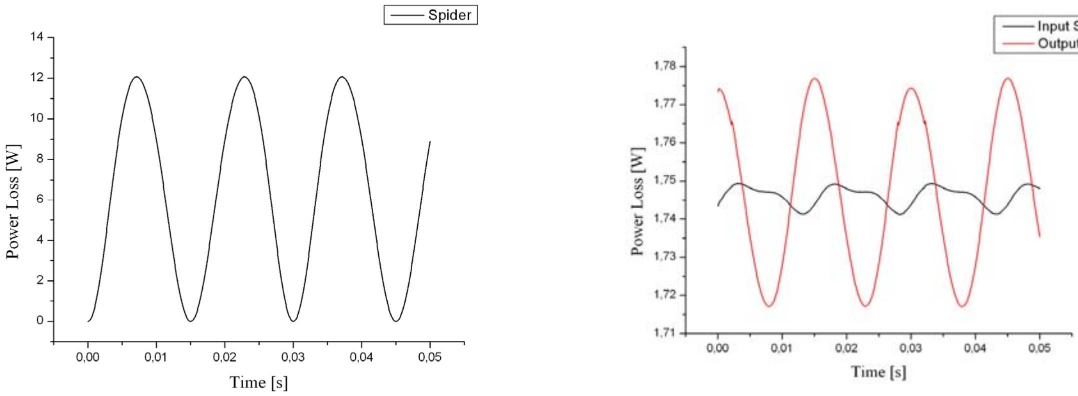


Figure 5: Power loss at the kinematic pairs of the spider (left) and of the shafts (right)

In Figure 5 the power loss at the kinematic pairs is shown. On the left there is the power loss at the kinematic pairs of the spider which has the fluctuation of the relative angular velocities between spider and shaft respectively. On the right hand side of Figure 5 the comparison between the power loss at the input and the output shaft is reported. The higher values at the output link are due to the angular configuration of the Cardan joint which affects the output angular velocity too. The fluctuation at input is caused by the eccentricity of centre of mass of the shaft.

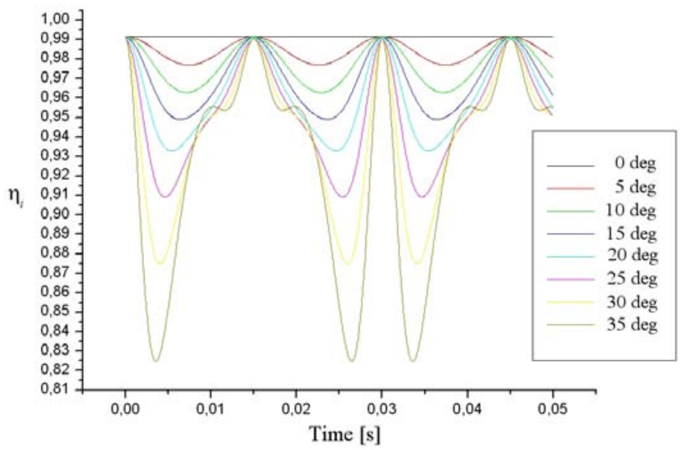


Figure 6: Comparison of mechanical efficiency for different configurations

Following the same criterion a comparison between the mechanical efficiencies at different configurations of the Cardan joint has been conducted. In Figure 6 the plots concerning this investigation are reported. The intersections between plots of Figure 6 could be explained considering that the plot at 35 deg is drastically influenced by inertial effects at such configuration and moreover that the plots represent the *instantaneous* mechanical efficiency of the joint. In fact the mean values of mechanical power loss increase with the increment of angular configuration (Table 2).

| Angular Configuration [deg] | Mean Value |
|---|---|
| 0 | 0.992 |
| 5 | 0.984 |
| 10 | 0.977 |
| 15 | 0.970 |
| 20 | 0.962 |
| 25 | 0.950 |
| 30 | 0.936 |
| 35 | 0.907 |

Table 2: Mechanical efficiency mean values

The influence of angular velocity on mechanical efficiency is also investigated. The angular displacement for this test case is 10 deg. Figure 7 shows the decrease of efficiency with the increase of angular speed.

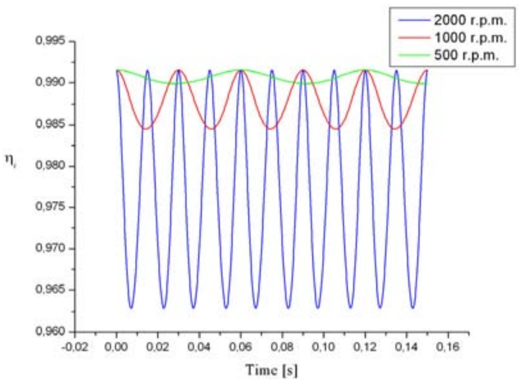


Figure 7: Comparison of mechanical efficiency for different angular speeds

The angular velocities considered are 500 r.p.m., 1000 r.p.m. and 2000 r.p.m., the corresponding mean values of mechanical efficiency are 0.991, 0.988 and 0.977 respectively.

## 4.2 Dual algebra approach results

The proposed approach has been validated by means of experimental tests. At the Laboratory of the Department of Mechanical Engineering of University of Rome Tor Vergata a test rig has been built up for this purpose (Figure 9).

Acting on motor virtual control panel and choosing the desired resisting torque exerted by the brake it is possible to simulate different working scenarios. Moreover, it is possible to simulate angular misalignment of the investigated joint tilting one end of the test rig.

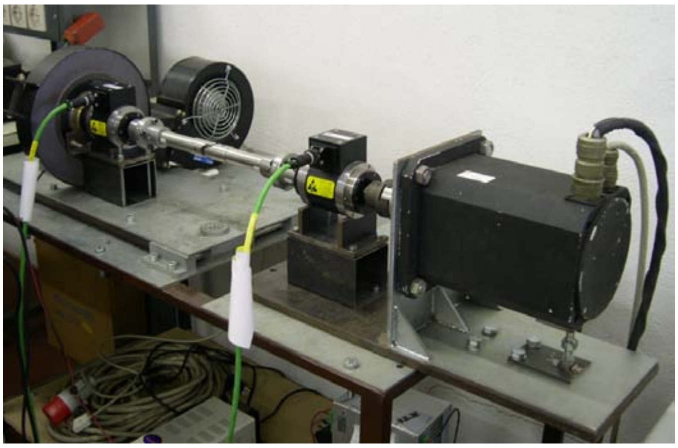

Figure 9: Experimental test rig

The test rig is equipped with the following instruments:

- an adjustable steel table;
- two torque/speed transducers (model Magtrol TMB 210 with max torque: 100.00 Nm; max speed: 4000 r.p.m.; torque sensitivity 100mV/Nm; speed sensitivity: 60 pulses per rev.);
- one brushless motor (two poles; peak torque: 110 Nm) with a control panel and control software;
- one electromagnetic brake (model Merobel SA FRAT 650; max torque 65 Nm; min torque 0.63 Nm) with a radial fan and a DGT 200 MC digital controller;
- one personal computer with an a/d converter and a National Instrument multi-channel acquiring system.

For this kind of analysis the implemented code (see [10,11]) has been modified in order to use the data acquired from the transducers. In particular the input torque and the input angular position, velocity and acceleration have been used. The acquired data have been filtered in order to reduce noise. The average values of torque and angular speed on input are 0.2 Nm and 6 rad/s respectively. The angular configuration of the Cardan joint is 15° and the dynamic friction coefficient is set equal to 0.42 for each kinematic pair. The manufacturing tolerances concerning the misalignment of the axes of the kinematic pairs are set in $a_i = 0.5\,\text{mm}$ (*i=1,2,3*) and the angular errors on $\alpha_i$ (*i=1,2,3*) are equal to $6 \cdot 10^{-3}$ deg. In Figure 10 the comparison between the experimental mechanical efficiency and the computed one is reported. Even if two different ways for evaluating the instantaneous mechanical efficiency[2] have been necessarily used, the results fit quite well.

Paper [11] reports in details the influence of dimensional tolerances and mounting errors on the mechanical efficiency of a Cardan joint.

[2] The instantaneous mechanical efficiency by means of the experimental data is obtained evaluating the input and output power. Instead the code estimates the output power computing the power loss at the kinematic pairs.

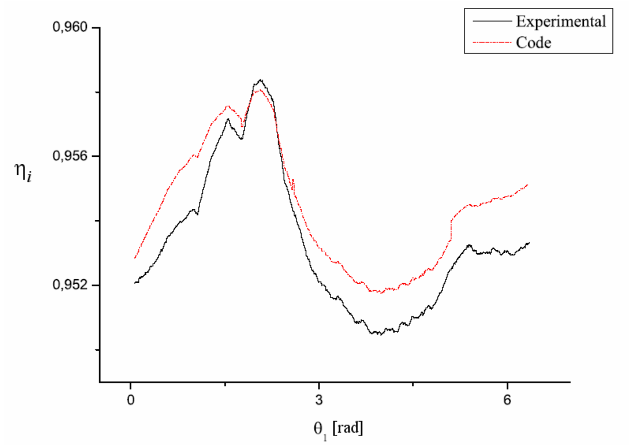


Figure 10: Comparison between the experimental and the computed mechanical efficiency

## 5 CONCLUSIONS

The authors presented a multibody dynamic model of a Cardan joint for the evaluation of the instantaneous mechanical efficiency. Two different approaches have been proposed. The first, based on the classical multibody methodology [7], has been used for the evaluation of the influence of angular configuration and angular speed on the mechanical efficiency. The second, based on the dual algebra [8,9], allowed to model clearances in the kinematic pairs and consequently to evaluate their influence on the mechanical efficiency. For both of the methodologies herein illustrated the effects of friction have been included. The results reported show that an increase of angular velocity makes the mechanical efficiency decrease of 1.4%; an increment of the angle between the input and the output shafts of the Cardan joint causes a reduction of mechanical yield of 8.6%. Both of the behaviors could be explained with an increase of friction effects at the kinematic pairs. These are more evident in concurrence with a considerable inclination of the Cardan joint where the inertial effects are more relevant. The presence of small dimensional errors does not affect so much the mechanical efficiency (0.15%). This is due to the not so relevant variation of the equilibrium condition at the kinematic pairs caused by clearances [10,11]. Moreover an experimental test rig has been built up and the results obtained have been successfully compared with the computed one.

## 6 ACKNOWLEDGEMENTS

The authors wish to acknowledge the grant by Ministry for Education, University and Research (MIUR).

## REFERENCES

[1] Fischer, I., Freudenstein, F., Internal Force and Moment Transmission in a Cardan Joint with Manufacturing Tolerances, *ASME Journal of Mechanisms, Transmissions and Automation in Design*, **106**, 301 – 311, December 1984.

[2] Chen, C.K., Freudenstein, F., Dynamic Analysis of a Universal Joint with Manufacturing Tolerances, *ASME Journal of Mechanisms, Transmissions and Automation in Design*, **108**, 524 – 532, December 1986.

[3] Freudenstein, F., Macey, J.P., The Inertia Torques of the Hooke Joint, *Proc. Of the 21st Biennial ASME Mechanisms Conference*, **24**, 407 – 413, Chicago, 1990.

[4] Duditza, F., *Transmissions par Cardan*, Editions Eyrolles, Paris, 1971.

[5] Shih C.W., Shih M.Y., Haug E.J., *Dynamics of Mechanical Systems with Coulomb Friction, Stiction, Impact and Constraint Deletion* - III, Mechanism and Machine Theory, **21**, pp.417-425, 1986.

[6] Dhanaraj C., Sharan A.M., *Efficient Modeling of Rigid Link Body Dynamic Problems with Friction*, Mechanism and Machine Theory, **30**, pp.749-764, 1995.

[7] E. J. Haug, *Computer- Aided Kinematics and Dynamics of Mechanical Systems*, vol.I, Allyn and Bacon, 1989.

[8] Fischer, I.S., *Dual-Number Methods in Kinematics, Statics and Dynamics*, CRC Press, Boca Raton, 1998.

[9] Yang, A.T., *Application of Quaternion Algebra and Dual Numbers to the Analysis of Spatial Mechanisms*, Doctoral Dissertation, Columbia University, New York, 1963.

[10] E. Pennestrì, L. Vita, *Mechanical Efficiency Analysis of a Cardan Joint with Manufacturing Tolerances*, Proceedings RAAD 2003 12th International Workshop on Robotics, Cassino 7-10 maggio, 2003

[11] M. Cavacece, E. Pennestrì, P.P. Valentini, L. Vita, Mechanical Efficiency Analysis of a Cardan Joint, *Proceedings of 2004 ASME Conference*, Salt Lake City, Utah, USA, September 28-October 2, 2004.

[12] E. Hairer, G. Wanner, *Solving Ordinary Differential Equations II: Stiff and Differential-algebraic Problems*, Springer-Verlag, Berlin Heidelberg New York, 1996.